

# Bistable firing pattern in a neural network model

February 1, 2022

P. R. Protachevicz<sup>1</sup>, F. S. Borges<sup>2</sup>, E. L. Lameu<sup>3</sup>, P. Ji<sup>4,5</sup>, K. C. Iarosz<sup>6</sup>,  
A. H. Kihara<sup>2</sup>, I. L. Caldas<sup>6</sup>, J. D. Szezech Jr.<sup>1,7</sup>, M. S. Baptista<sup>8</sup>, E. E. N.  
Macau<sup>3</sup>, C. G. Antonopoulos<sup>9</sup>, A. M. Batista<sup>1,7</sup>, J. Kurths<sup>10,11,\*</sup>

<sup>1</sup>Graduate in Science Program - Physics, State University of Ponta Grossa, PR, Brazil

<sup>2</sup>Center for Mathematics, Computation, and Cognition, Federal University of ABC, São Bernardo do Campo, SP, Brazil

<sup>3</sup>National Institute for Space Research, São José dos Campos, SP, Brazil

<sup>4</sup>Institute of Science and Technology for Brain-Inspired Intelligence, Fudan University, Shanghai, China

<sup>5</sup>Key Laboratory of Computational Neuroscience and Brain-Inspired Intelligence (Fudan University), Ministry of Education, China

<sup>6</sup>Institute of Physics, University of São Paulo, São Paulo, SP, Brazil

<sup>7</sup>Department of Mathematics and Statistics, State University of Ponta Grossa, Ponta Grossa, PR, Brazil

<sup>8</sup>Institute for Complex Systems and Mathematical Biology, SUPA, University of Aberdeen, Aberdeen, AB24 3UE, Scotland, United Kingdom

<sup>9</sup>Department of Mathematical Sciences, University of Essex, Wivenhoe Park, UK

<sup>10</sup>Potsdam Institute for Climate Impact Research, Potsdam, Germany

<sup>11</sup>Department of Physics, Humboldt University, Berlin, Germany Jürgen Kurths kurths@pik-potsdam.de

## Abstract

Excessively high, neural synchronisation has been associated with epileptic seizures, one of the most common brain diseases worldwide. A better understanding of neural synchronisation mechanisms can thus help control or even

treat epilepsy. In this paper, we study neural synchronisation in a random network where nodes are neurons with excitatory and inhibitory synapses, and neural activity for each node is provided by the adaptive exponential integrate-and-fire model. In this framework, we verify that the decrease in the influence of inhibition can generate synchronisation originating from a pattern of desynchronised spikes. The transition from desynchronous spikes to synchronous bursts of activity, induced by varying the synaptic coupling, emerges in a hysteresis loop due to bistability where abnormal (excessively high synchronous) regimes exist. We verify that, for parameters in the bistability regime, a square current pulse can trigger excessively high (abnormal) synchronisation, a process that can reproduce features of epileptic seizures. Then, we show that it is possible to suppress such abnormal synchronisation by applying a small-amplitude external current on less than 10% of the neurons in the network. Our results demonstrate that external electrical stimulation not only can trigger synchronous behaviour, but more importantly, it can be used as a means to reduce abnormal synchronisation and thus, control or treat effectively epileptic seizures.

Keywords: bistable regime, network, adaptive exponential integrate-and-fire neural model, neural dynamics, synchronisation, epilepsy

## 1 Introduction

Epilepsy is a brain disease that causes seizures and sometimes loss of consciousness [7, 6]. Epileptic seizures are associated with excessively high synchronous activities [26, 22, 52] of neocortex regions or other neural populations [16, 38, 14, 17, 15]. Electroencephalography has been used to identify and classify seizures [31], as well as to understand epileptic seizures [36]. Abnormal activities have a short period of time, lasting from a few seconds to minutes [45], and they can occur in small or larger regions in the brain [28, 24]. Two suggested mechanisms responsible for the generation of partial epilepsy are the decrease of inhibition and increase of excitation [28]. In experiments and simulations, the reduction of excitatory and the increase of inhibitory influence have been effective in suppressing and preventing synchronised behaviours [43, 37]. Traub and Wong [44] showed that synchronised bursts that appear in epileptic seizures depend on neural dynamics.

Single seizures can not kill neurons, however recurrent ones can do so and thus, can lead to chronic epilepsy [13]. Evidence that supports this further is provided by abnormal anatomical alterations, such as mossy fiber sprouting [12], dendritic reconfigurations [50, 51], and neurogenesis [21, 8].

In fact, such alterations change the balance between inhibition and excitation [20, 39]. Wang et al. [48] demonstrated that a small alteration in the network topology can induce a bistable state with an abrupt transition to synchronisation. Some *in vitro* seizures generated epileptiform activities when inhibitory synapses were blocked or excitatory synapses were enhanced [42, 49]. Several studies showed that epileptiform activities are related not only with unbalanced neural networks, but also with highly synchronous regimes [46, 1].

Different routes to epileptic seizures were reported by Silva et al. [39]. The authors considered epilepsy as a dynamical disease and presented a theoretical framework where epileptic seizures occur in neural networks that exhibit bistable dynamics. In the bistable state, transitions can happen between desynchronous and synchronous behaviours. Suffczynski et al. [40] modelled the dynamics of epileptic phenomena by means of a bistable network.

Many works reported that periodic electrical pulse stimulation facilitates synchronisation, while random stimulation promotes desynchronisation in networks [10]. Electrical stimulation can be applied in different brain areas, for instance in the hippocampus, thalamus, and cerebellum [28]. The mechanism for electrical stimulation to cease seizures is still not completely understood, however, signal parameters such as frequency, duration and amplitude can be changed to improve the efficiency of the treatment of epilepsy [28]. The electrical stimulation has been used as an efficient treatment for epilepsy in the hippocampus [47]. In [2], the author studied external electrical perturbations and their responses in the brain dynamic network of the *Caenorhabditis elegans* soil worm. It was shown that when one perturbs specific communities, keeping the others unperturbed, the external stimulations propagate to some but not all of them. It was also found that there are perturbations that do not trigger any response at all and that this depends on the initially perturbed community.

Neural network models have been used to mimic phenomena related to neural activities in the brain. Guo et al. [19] built a network model where the postsynaptic neuron receives input from excitatory presynaptic neurons. They incorporated autaptic coupling [18] in a biophysical model. Delayed models have been considered in biological systems [23], for instance, Sun et al. [41] analysed the influence of time delay in neuronal networks. They showed that intra- and inter-time delays can induce fast regular firings in clustered networks. In this work, we build a random network with neural dynamics to study synchronisation induced in a bistable state which is related to epileptic seizures. In particular, we consider a network composed of adaptive exponential integrate-and-fire (AEIF) neurons coupled by means of inhibitory and excitatory synapses. The AEIF model mimics phenomenologi-

cal behaviours of neurons [9] and is appropriate to study even large networks [29]. Borges et al. [4] verified that depending on the excitatory synaptic strength and connection probability, a random network of coupled AEIF neurons can exhibit transitions between desynchronised spikes and synchronised bursts [33]. In the network considered here, we observe the existence of bistability when it is unbalanced, namely that the decrease of synaptic inhibition induces a bistable state. We analyse the effects of the application of external square current pulses (SCP) by perturbing the neural dynamics on the network using parameters that lead to a bistable state, such as the excitatory and inhibitory synaptic conductances. We find that, depending on the duration and amplitude of the external current, SCP can either trigger or suppress synchronisation in the bistability region, an idea that can be used further to treat epilepsy by suppressing excessive synchronisation in affected brain regions.

## 2 Methods

### 2.1 Neural network model

We build a random network of  $N = 1000$  adaptive exponential integrate-and-fire neurons [5] with probability  $p$  for the formation of connections among them equal to 0.1. The network consists of 80% excitatory and 20% inhibitory neurons [30]. The dynamics of each neuron  $i$ ,  $i = 1, \dots, N$  in the network is given by the set of equations

$$\begin{aligned}
C_m \frac{dV_i}{dt} &= -g_L(V_i - E_L) + g_L \Delta_T \exp\left(\frac{V_i - V_T}{\Delta_T}\right) \\
&+ I_i - w_i + \sum_{j=1}^N (V_{\text{REV}}^j - V_i) M_{ij} g_j + \Gamma_i, \\
\tau_w \frac{dw_i}{dt} &= a_i(V_i - E_L) - w_i, \\
\tau_s \frac{dg_i}{dt} &= -g_i.
\end{aligned} \tag{1}$$

The membrane potential  $V_i$  and adaptation current  $w_i$  represent the state of each neuron  $i$ . The capacitance membrane  $C_m$  is set to  $C_m = 200\text{pF}$ , the leak conductance to  $g_L = 12\text{ns}$ , the resting potential to  $E_L = -70\text{mV}$ , the slope factor to  $\Delta_T = 2.0\text{mV}$  and the spike threshold to  $V_T = -50\text{mV}$ . The adaptation current depends on the adaptation time constant  $\tau_w = 300\text{ms}$  and the level of subthreshold adaptation  $a_i$  that is randomly distributed in



the interval  $[0.19, 0.21]$ ns. We consider the injection of current  $I_i$  to each neuron  $i$  in terms of the relative rheobase current  $r_i = I_i/I_{\text{rheobase}}$  [29]. The rheobase is the minimum amplitude of the applied current to generate a single or successive firings. The application of this constant current allows neurons to change their potentials from resting potentials to spikes. The value of the rheobase depends on the neuron parameters. The external current arriving at neuron  $i$  is represented by  $\Gamma_i$ . We consider the external current according to a SCP with amplitude  $A_I$  and time duration  $T_I$ . The random connections in the network are described by the binary adjacency matrix  $M_{ij}$  with entries either equal to 1 when there is a connection from  $i$  to  $j$  or 0 in the absence of such a connection.  $g_i$  is the synaptic conductance,  $\tau_s$  the synaptic time constant, and  $V_{\text{REV}}$  the synaptic reversal potential. We consider  $\tau_s = 2.728$ ms,  $V_{\text{REV}} = 0$ mV for excitatory synapses, and  $V_{\text{REV}} = -80$ mV for inhibitory synapses. The synaptic conductance decays exponential with a synaptic time constant  $\tau_s$ . When the membrane potential of neuron  $i$  is above the threshold  $V_i > V_{\text{thres}}$  [29], the state variable is updated by the rule

$$\begin{aligned} V_i &\rightarrow V_r = -58\text{mV}, \\ w_i &\rightarrow w_i + 70\text{pA}, \\ g_i &\rightarrow g_i + g_s, \end{aligned} \tag{2}$$

where  $g_s$  assumes the value of  $g_{\text{exc}}$  when neuron  $i$  is excitatory ( $i \leq 0.8N$ ) and  $g_{\text{inh}}$  when neuron  $i$  is inhibitory ( $i > 0.8N$ ). In this work, we study the parameter space  $(g_{\text{exc}}, g_{\text{inh}})$  and consider a relative inhibitory synaptic conductance  $g = g_{\text{inh}}/g_{\text{exc}}$ . We consider parameter values in which the individual uncoupled neurons perform spike activities. The initial values of  $V$  and  $w$  are randomly distributed in the interval  $[-70, -50]$ mV and  $[0, 70]$ pA, respectively. The initial  $g_i$  value is equal to 0.

## 2.2 Synchronisation

The synchronous behaviour in the network can be identified by means of the complex phase order parameter [25]

$$R(t) \exp(i\Phi(t)) \equiv \frac{1}{N} \sum_{j=1}^N \exp(i\psi_j(t)), \tag{3}$$

where  $R(t)$  and  $\Phi(t)$  are the amplitude and angle of a centroid phase vector over time, respectively. The phase of neuron  $j$  is obtained by means of

$$\psi_j(t) = 2\pi m + 2\pi \frac{t - t_{j,m}}{t_{j,m+1} - t_{j,m}}, \tag{4}$$

where  $t_{j,m}$  corresponds to the time of the  $m$ -th spike of neuron  $j$  ( $t_{j,m} < t < t_{j,m+1}$ ) [34, 35]. We consider that the spike occurs for  $V_j > V_{\text{thres}}$ .  $R(t)$  is equal to 0 for fully desynchronised and 1 for fully synchronised patterns, respectively.

We calculate the time-average order parameter  $\overline{R}$  [3] given by

$$\overline{R} = \frac{1}{t_{\text{fin}} - t_{\text{ini}}} \int_{t_{\text{ini}}}^{t_{\text{fin}}} R(t) dt, \quad (5)$$

where  $t_{\text{fin}} - t_{\text{ini}}$  is the time window. We consider  $t_{\text{fin}}=200\text{s}$  and  $t_{\text{ini}}=180\text{s}$ .

## 2.3 Synaptic input

We monitor the instantaneous synaptic conductances arriving at each neuron  $i$  through

$$I_i^{\text{ISC}}(t) = \sum_{j=1}^N (V_{\text{REV}}^j - V_i) M_{ij} g_j. \quad (6)$$

The instantaneous synaptic input changes over time due to the excitatory and inhibitory inputs received by neuron  $i$ . The average instantaneous synaptic conductances is given by

$$I_{\text{syn}}(t) = \frac{1}{N} \sum_{i=1}^N I_i^{\text{ISC}}(t). \quad (7)$$

## 2.4 Coefficient of variation

The  $m$ -th inter-spike interval  $\text{ISI}_i^m$  is defined as the difference between two consecutive spikes of neuron  $i$ ,

$$\text{ISI}_i^m = t_i^{m+1} - t_i^m > 0, \quad (8)$$

where  $t_i^m$  is the time of the  $m$ -th spike of neuron  $i$ .

Using the mean value of  $\text{ISI}_i$ ,  $\overline{\text{ISI}}_i$ , and its standard deviation,  $\sigma_{\text{ISI}_i}$ , we calculate the coefficient of variation (CV)

$$\text{CV}_i = \frac{\sigma_{\text{ISI}_i}}{\overline{\text{ISI}}_i}. \quad (9)$$

The average of CV ( $\overline{\text{CV}}$ ) is then obtained through

$$\overline{\text{CV}} = \frac{1}{N} \sum_{i=1}^N \text{CV}_i. \quad (10)$$

Finally, we use  $\overline{\text{CV}}$  to identify spike (when  $\overline{\text{CV}} < 0.5$ ) and burst fire patterns (when  $\overline{\text{CV}} \geq 0.5$ ) [4, 33].

## 2.5 Instantaneous and mean firing-rate

The instantaneous firing-rate in intervals of  $t_{\text{step}} = 1\text{ms}$  is given by

$$F(t) = \frac{1}{N} \sum_{i=1}^N \left( \int_t^{t+t_{\text{step}}} \delta(t' - t_i) dt' \right), \quad (11)$$

where  $t_i$  is the firing time of neuron  $i$  in the time interval  $(t \leq t_i \leq t + 1)\text{ms}$ . This measure allows to obtain the instantaneous population activity in the network. The mean firing-rate can then be calculated by means of

$$\overline{F} = \frac{1}{\overline{\text{ISI}}}, \quad (12)$$

where  $\overline{\text{ISI}}$  is the average ISI obtained over all  $N$  neurons in the network, that is  $\overline{\text{ISI}} = \frac{1}{N} \sum_{i=1}^N \overline{\text{ISI}}_i$ .

## 3 Results

### 3.1 Inhibitory effect on synchronous behaviour

The balance between excitation and inhibition generates an asynchronous activity in the network [27, 32]. However, for the unbalanced network we observe synchronised spikes and bursts. Figures 1(a), 1(b), and 1(c) show the time-average order parameter ( $\overline{R}$ ), the mean coefficient of variation ( $\overline{\text{CV}}$ ) and the mean firing-rate ( $\overline{F}$ ), respectively, for the parameter space  $(g, r)$ , where  $g$  is the ratio between inhibitory ( $g_{\text{inh}}$ ) and excitatory ( $g_{\text{exc}}$ ) synaptic conductances, and  $r$  the relative rheobase current. For  $g_{\text{exc}} = 0.4\text{ns}$  and  $g > 6$ , we observe that  $\overline{R} < 0.5$  and that  $\overline{\text{CV}} < 0.5$ , corresponding to desynchronised spikes. In Fig. 1(d), we see the raster plot and membrane potential for 2 neurons in the network with a desynchronised spike-pattern for  $g = 5.5$  and  $r = 2$  (blue triangle). For  $g = 4$  and  $r = 1.5$  (magenta square), the dynamics exhibits synchronised spikes (Fig. 1(e)), as a result of setting  $\overline{R} > 0.9$  and  $\overline{\text{CV}} < 0.5$ . Figure 1(f) shows synchronised bursts of activity for  $g = 2.5$  and  $r = 2$  (green circle), where  $\overline{R} > 0.9$  and  $\overline{\text{CV}} \geq 0.5$ . Within this framework, we have verified the existence of transitions from desynchronised spikes to synchronised bursting activities without significant changes in the mean firing-rate.

The appearance of synchronous behaviour cannot only be related to the decrease of the inhibitory synaptic strength, but also to a loss of inhibitory neurons. In particular, we show this in Fig. 1(g) which illustrates a network

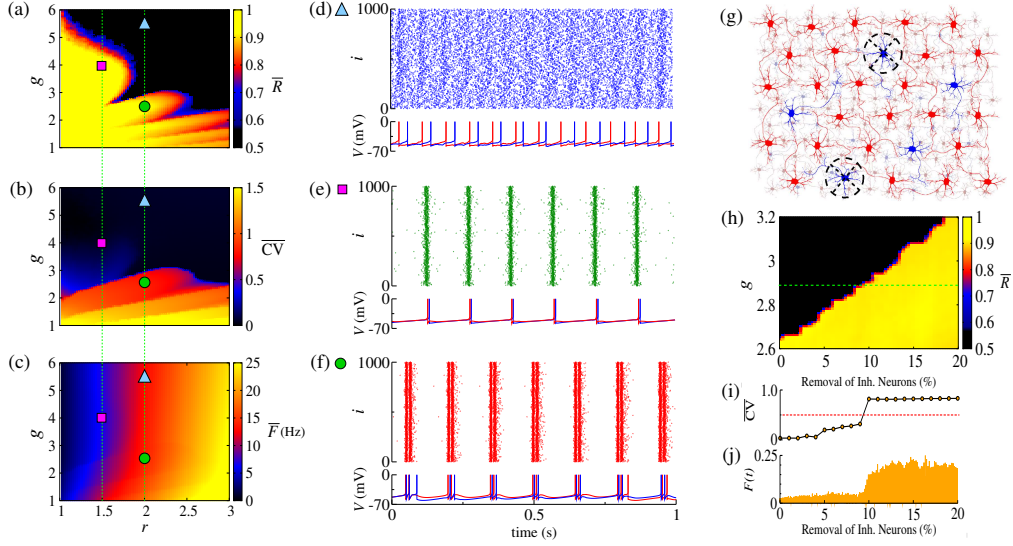


Figure 1: (Colour online) Parameter space  $(g, r)$  for the (a) time-average order parameter  $\overline{R}$ , (b) the mean coefficient of variation  $\overline{CV}$ , and (c) the mean firing-rate  $\overline{F}$ . Raster plot that displays the spiking activity over time and membrane potential are shown for (d) desynchronised spikes for  $r = 2.0$  and  $g = 5.5$  (cyan triangle), (e) synchronised spikes for  $r = 1.5$  and  $g = 4$  (magenta square), and (f) synchronised bursts for  $r = 2.0$  and  $g = 2.5$  (green circle). Here, we consider  $g_{\text{exc}} = 0.4\text{ns}$ . In panel (g), we illustrate a network composed of excitatory (red) and inhibitory (blue) neurons, where some inhibitory neurons are removed (black dashed circle). Figure (h) shows the time-average order parameter for  $g$  versus the percentage of inhibitory neurons removed from the network. The green dashed line corresponds to  $g = 2.9$ . The values of  $\overline{CV}$  and instantaneous firing-rate are shown in panels (i) and (j), respectively.

composed of excitatory (red) and inhibitory (blue) neurons, where some inhibitory neurons were removed (dashed circles). In Fig. 1(h), we see that the synchronous behaviour depends on  $g$  and the percentage of removed inhibitory neurons. Figure 1(i) shows the transition from spiking dynamics ( $\overline{CV} < 0.5$ ) to bursting dynamics ( $\overline{CV} \geq 0.5$ ), and Fig. 1(j) shows the instantaneous firing-rate  $F(t)$ . For  $g = 2.9$  and  $g_{\text{exc}} = 0.4\text{ns}$  (green dashed line), the transition to synchronised bursts occurs when approximately 10% of inhibitory neurons are removed from the network, and as a consequence  $F(t)$  reaches the maximum value of 0.2.

Concluding, alterations in the inhibitory synaptic strength or in the number of inhibitory neurons can induce transition to synchronous patterns.

Wang et al. [48] presented results where synchronisation transition occurs as a result of small changes in the topology of the network, whereas here, we study transitions caused due to changes in the inhibitory synaptic strength and the emergence of a bistable regime.

### 3.2 Bistable regime

Next, we analyse synchronisation in the parameter space  $(g, g_{\text{exc}})$ . In particular, Fig. 2(a) shows  $\bar{R}$  with values depicted in the colour bar. The black region corresponds to desynchronised spike activity, while the remaining coloured regions are associated with burst activities. The white region represents the bistable regime, where desynchronised spikes or synchronised bursts are possible depending on the initial conditions. In the bistable regime, decreasing  $g_{\text{exc}}$  (backward direction),  $\bar{R}$  is higher than increasing  $g_{\text{exc}}$  (forward direction), as shown in Fig. 2(b) for  $g = 3$ ,  $r = 2$ , and  $g_{\text{exc}} = [0.35, 0.45]\text{ns}$  (green dashed line in Fig. 2(a)). We identify bistability (white region) in the parameter space when the condition  $\bar{R}_{\text{backward}} - \bar{R}_{\text{forward}} > 0.4$  is fulfilled. The raster plot and instantaneous synaptic input for desynchronised spikes (blue circle) and synchronised bursts (red square) are shown in Figs. 2(c) and 2(d), respectively. When the dynamics on the random network is characterised by desynchronised spikes, the instantaneous synaptic inputs exhibit  $I_{\text{syn}}(t) \approx 50\text{pA}$ . For synchronised bursts,  $I_{\text{syn}}(t) \approx 0$  when a large number of neurons in the network are silent (i.e. not firing), and  $I_{\text{syn}}(t) > 200\text{pA}$  during synchronous firing activities. In Fig. 2(e), we compute the probability of occurrence of excessively high synchronicity within the bistable regime. We observe a small synchronisation probability value in the bistable region. This result has a biological importance due to the fact that the seizure state is a relatively small probability event compared with the normal state. DaQing et al. [11] showed that noise can regulate seizure dynamics in partial epilepsy. Figure 2(f) displays  $\bar{R} \times g_{\text{exc}}$  for Gaussian noise with mean 0 and standard deviation  $\sigma_{\text{noise}}$  equal to 25pA and 250pA. We verify that the bistable region decreases when the noise level increases.

In the bistable regime, we investigate the evolution of a trajectory for a finite time interval in the phase space  $(w_i, V_i)$  and the time evolution of  $w_i$  shown in Fig. 3 for  $i = 1$ , where the grey regions correspond to  $dV_i/dt < 0$ . The boundary between the grey and white regions (black line) is given by  $dV_i/dt = 0$ , the  $V_i$ -nullcline [29]. During spiking activity, the trajectory (see Fig. 3(a)) and time evolution of  $w_i$  (see Fig. 3(b)) do not cross the  $V_i$ -nullcline. For bursting activities (see Figs. 3(c) and 3(d)), we observe that  $w_i$  lies in the region enclosed by the  $V_i$ -nullcline. The emergence of the bistable behaviour is related to changes in the  $V_i$ -nullcline caused by the variation of

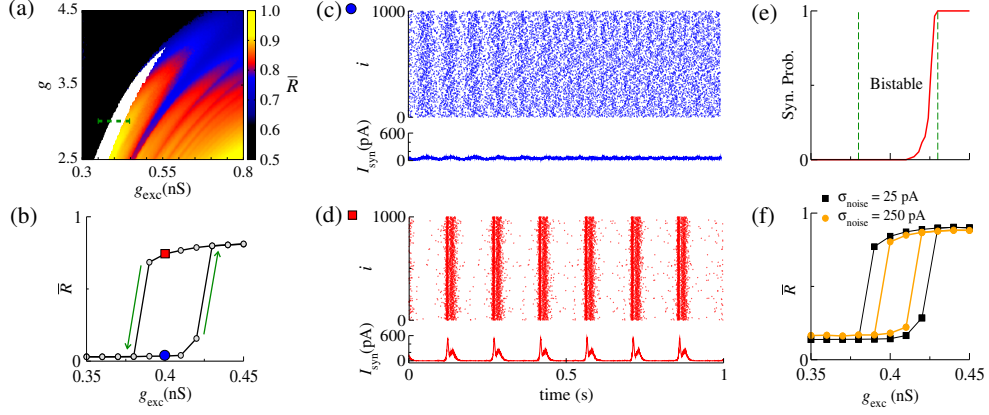


Figure 2: (Colour online) (a) The parameter space  $(g, g_{\text{exc}})$  for  $r = 2$ , where  $\bar{R}$  is encoded in colour. The black region corresponds to desynchronised activity, whereas coloured regions indicate  $\bar{R} > 0.6$  and the white region represents the bistable regime. (b) The bistable region indicated in the parameter space of (a) by means of a green dashed line. Panels (c) and (d) show the raster plots and  $I_{\text{syn}}$  for desynchronised spikes (blue circle) and synchronised bursts (red square), respectively. We identify bistability by checking when  $\bar{R}_{\text{backward}} - \bar{R}_{\text{forward}} > 0.4$  and consider two trials for each set of parameter values. (e) The synchronisation probability as a function of  $g_{\text{exc}}$ . (f)  $\bar{R} \times g_{\text{exc}}$  for  $\sigma_{\text{noise}}$  equal to 25pA and 250pA.

$I_{\text{syn}}$ .

### 3.3 External square current pulse

Here, following a similar idea as in [2], we investigate the effect of the application of SCP on the bistable regime. We apply SCP considering different values of  $A_I$ ,  $T_I$ , and number of removed inhibitory neurons. The SCP is immediately switched off after  $T_I$  and the analysis of the effect on the dynamical behaviour is started.

Initially, we apply SCP to all neurons in the network with parameter values in the bistable regime with desynchronous behaviour (white region in Fig. 2(a)). Figure 4(a) displays the time (in colour scale) that the neurons show a synchronised pattern after the application of SCP. In the black region, we see that SCP does not change the dynamical behaviour, namely the neurons remain in a regime of desynchronised behaviour. The yellow region depicts the values of  $T_I$  and  $A_I$  of the SCP that induce a change in the behaviour of the neurons from desynchronised spikes to synchronised bursts.

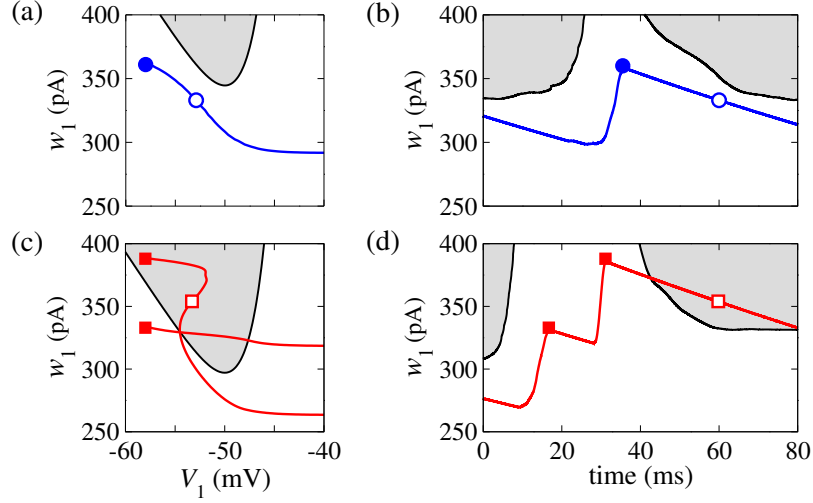


Figure 3: (Colour online) Phase space  $(w_1, V_1)$  ((a) and (c)) and time evolution of  $w_1$  ((b) and (d)) for spikes (blue) and burst activity (red). The grey regions correspond to  $dV_1/dt < 0$  and the black line represents  $dV_1/dt = 0$  ( $V$ -nullcline).

Picking up one point close to the border of the black and blue regions (white circle), we see that the instantaneous firing-rate ( $F(t)$ ) of Eq. 11 (see Fig. 4(b), blue line) exhibits low-amplitude oscillations corresponding to desynchronised spikes. For  $T_I$  and  $A_I$  values in the yellow region,  $F(t)$  (see Fig. 4(c), red line) exhibits a high-amplitude oscillation after the application of SCP, corresponding to synchronised bursts. For sufficiently large amplitudes, the change in the behaviour induced by SCP does not depend on time. Importantly, perturbations with small amplitudes applied for short times is a sufficient condition for the induction of synchronous burst activity in the bistable regime. Therefore, our results suggest that even small excitatory stimuli in a random neural network arriving from other parts might be sufficient for the initiation of excessively high neural synchronisation, related to the onset of epileptic seizures. Thus, further work on other neural networks that resemble brain activity might provide more insights on epileptogenesis.

Similarly, we apply SCP when the neurons in the network show synchronised bursts of firing activity in the bistable regime. Here, we aim to suppressing the synchronous behaviour by means of applying SCP. We consider SCP with positive and negative amplitudes applied to 10% of the neurons in the random network. Figure 5(a) shows how long the bursts remain synchronised after SCP is switched off (colour bar). We verified that both negative and positive amplitudes exhibit regions where the synchronous behaviours

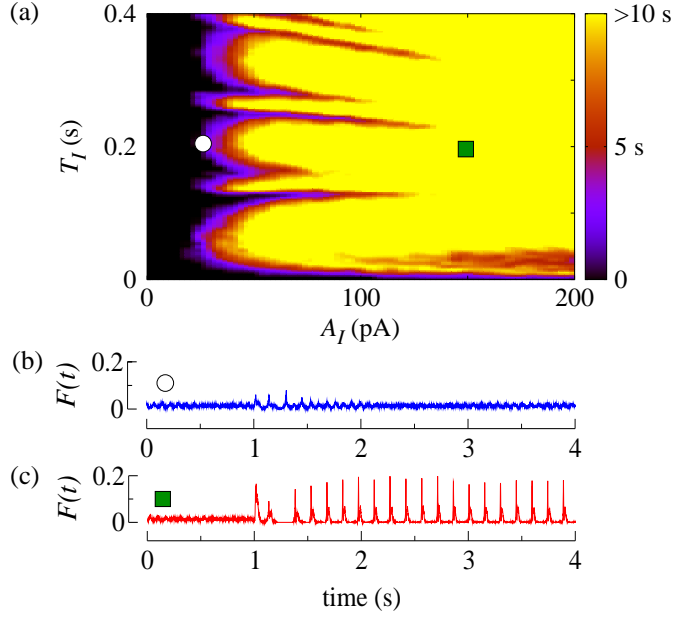


Figure 4: (Colour online) (a) The parameter space  $(T_I, A_I)$  in the bistable regime, where the colour bar indicates the time the system shows synchronised burst behaviour after the application of SCP. Instantaneous firing-rate for values for (b) white circle ( $A_I = 25$  pA,  $T_I = 0.2$  s) and (c) green square ( $A_I = 150$  pA,  $T_I = 0.2$  s). Note that in this figure  $g_{\text{exc}} = 0.4$  ns,  $g = 3$  and  $r = 2$ .

are suppressed, namely there is a transition from synchronised bursts to desynchronised spikes. In addition, for  $T_I > 0.4$  s and considering the absolute value of the amplitudes, the transition occurs for positive values with smaller amplitudes than for negative values. In Fig. 5(b), we show the dependence of the percentage of the perturbed neurons by the stimulus on the time the neurons remain in the bursting synchronous regime. The black region represents parameters for which the dynamics on the network does not remain synchronous, and therefore, synchronisation is suppressed. In this figure,  $T_I = 1$  s. These results allow us to conclude that desynchronous behaviour is achieved for  $A_I > 15$  pA and for at least 10% of the perturbed neurons.

## 4 Discussion and Conclusion

In this paper, we studied the influence of inhibitory synapses on the appearance of synchronised and desynchronised fire patterns in a random network



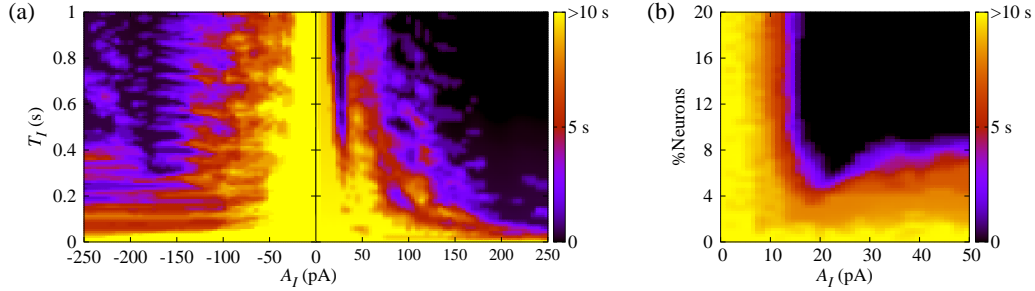


Figure 5: (Colour online) (a) The parameter space  $(T_I, A_I)$ , where the colour bar indicates the time the system shows synchronised burst behaviour after the application of SCP. (b) Number of perturbed neurons as a function of  $A_I$ . Note that in this figure we consider  $g_{exc} = 0.4ns$ ,  $g = 3$  and  $r = 2$ .

with adaptive exponential integrate-and-fire neural dynamics. When the inhibitory influence is reduced by either decreasing the inhibitory synaptic strength or the number of inhibitory neurons, the dynamics on the network is more likely to exhibit synchronous behaviour. The occurrence of synchronisation results from the lack of balance between excitatory and inhibitory synaptic influences.

We found parameter values that shift to a bistable regime where the neurons can either exhibit desynchronous spiking or synchronised bursting behaviour. In the bistability region, a desynchronous (synchronous) behaviour becomes synchronous (desynchronous) by varying forward (backward)  $g_{exc}$ . The onset of synchronisation is thus associated with a hysteresis-loop

We showed that, in the bistable regime, synchronised bursts can be induced by means of applying square current pulses. Our study also showed that outside the bistable regime, square current pulses do not induce synchronisation. Furthermore, in the bistable regime, when neurons are synchronised, square current pulses can be used to suppress it. Positive amplitudes of square current pulses are more effective in ceasing synchronised bursts than negative ones. In addition, we showed that when one applies square current pulses to less than 10% of the neurons in the network, it is enough to desynchronise the dynamics. Our work shows that a decrease of inhibition contributes to the appearance of excessively high synchronisation, reminiscent of the onset of epileptic seizures in the brain, thus confirming previous experimental results and theoretical models. Both decreasing the number of inhibitory neurons and the inhibitory strength, induce excessively high synchronisation, related to epilepsy.

Finally, within this framework, we hypothesise that low amplitude stimuli

coming from some brain regions might be capable of inducing an epileptic seizure manifested by high neural (abnormal) synchronisation in other brain regions. Therefore, the work in this paper supports the common approach of the induction of square current pulses to control or treat epileptic seizures, since we have shown that such external perturbations not only can induce, but more importantly can suppress synchronous behaviour in random networks with neural dynamics.

## Acknowledgments

This study was possible by partial financial support from the following Brazilian government agencies: Fundação Araucária, CNPq (433782/2016 – 1, 310124/2017–4, and 428388/2018–3), CAPES, and FAPESP (2015/50122–0, 2015/07311–7, 2016/16148–5, 2016/23398–8, 2017/13502–5, 2017/18977–1, 2018/03211 – 6). We also wish to thank the Newton Fund, COFAP, and International Visiting Fellowships Scheme of the University of Essex. We also thank IRTG for support.

## References

- [1] Abdullahi, A. T., & Adamu, L. H. (2017). Neural network models of epileptogenesis, *Neurosciences*, 22(2), 85-93.
- [2] Antonopoulos C. G. (2016). Dynamic range in the C.elegans brain network, *Chaos*, 26(1), 1054-1500.
- [3] Batista, C. A. S., Szezech Jr, J. D., Batista, A. M., Macau, E. E. N., & Viana, R. L. (2017). Synchronization of phase oscillators with coupling mediated by a diffusing substance, *Physica A*, 470, 236-248.
- [4] Borges, F. S., Protachevich, P. R., Lameu, E. L., Bonetti, R. C., Iarosz, K. C., Caldas, I. L., Baptista, M. S., & Batista., A. M. (2017). Synchronised firing patterns in a random network of adaptive exponential integrate-and-fire neuron model, *Neural Networks*, 90, 1-7.
- [5] Brette, R., & Gerstner, W. (2005). Adaptive exponential integrate-and-fire model as an effective description of neural activity, *Journal of Neurophysiology*, 94, 3637-3642.
- [6] Chen, M., Guo, D., Li, M., Ma, T., Wu, S., Ma, J., Cui, Y., Xu, P., & Yao, Y. (2015). Critical roles of the direct GABAergic pallido-cortical

- pathway in controlling absence seizures, *Plos Computational Biology*, 11(10), e1004539.
- [7] Chen, M., Guo, D., Wang, T., Jing, W., Xia, Y., Xu, P., Luo, C., Valdes-Sosa, P. A., & Yao, D. (2014). Bidirectional control of absenced seizures by the basal ganglia: A computational evidence, *Plos Computational Biology*, 10(3), e1003495.
  - [8] Cho, K.-O., Lybrand, Z. R., Ito, N., Brulet, R., Tafacory, F., Zhang, L., Good, L., Ure, K., Kernie, S. G., Birnbaum, S. G., Scharfman, H. E., Eisch, A. J., & Hsieh, J. (2015). Aberrant hippocampal neurogenesis contributes to epilepsy and associated cognitive decline, *Nature Communications*, 6, 6606.
  - [9] Clopath, C., Jolivet, R., Rauch, A., Lüscher, H.-R., & Gerstner, W. (2007). Predicting neural activity with simple models of the threshold type: adaptive exponential integrate-and-fire model with two compartments, *Neurocomputing*, 70(10-12), 1668-1673.
  - [10] Cota, V. R., Medeiros, D. C., Vilela, M. R. S. P., Doretto, M. C., & Moraes, M. F. D. (2009). Distinct patterns of electrical stimulation of the basolateral amygdala influence pentylentetrazole seizure outcome, *Epilepsy & Behavior*, 14, 26-31.
  - [11] DaQing, G., Chuan, X., ShengDun, W., TianJiao, Z., YangSong, Z., Yang, X., & DeZhong, Y. (2017). Stochastic fluctuations of permittivity coupling regulate seizure dynamics in partial epilepsy, *Science China Technological Sciences*, 60(7), 995-1002.
  - [12] Danzer, S. (2017). Mossy fiber sprouting in the epileptic brain: Taking on the Lernaean Hydra, *Epilepsy Currents*, 17(1), 50-51.
  - [13] Dingledine, R., Varvel, N. H., & Dudek, F. E. (2014). When and how do seizures kill neurons, and is cell death relevant to epileptogenesis? *Advances in Experimental Medicine and Biology*, 813, 109-122.
  - [14] Engel, J. Jr., Thompson, P. M., Stern, J. M., Staba, R. J., Bragin, A., & Mody, I. (2013). Connectomics and epilepsy, *Current Opinion in Neurology*, 26, 186-194.
  - [15] Falco-Walter, J. J., Scheffer, I. E., & Fisher, R. S. (2018). The new definition and classification of seizures and epilepsy, *Epilepsy Research*, 139, 73-79.

- [16] Fisher, R. S., van Emde Boas, W., Blume, W., Elger, C., Genton, P., Lee, P., & Engel, J. Jr. (2005). Epileptic seizures and epilepsy: Definitions proposed by the International League Against Epilepsy (ILAE) and the International Bureau for Epilepsy (IBE), *Epilepsia*, 46(4), 470-472.
- [17] Geier, C., & Lehnertz, K. (2017). Which Brain Regions are Important for Seizure Dynamics in Epileptic Networks? Influence of Link Identification and EEG Recording Montage on Node Centralities, *International Journal of Neural Systems*, 27, 1650033.
- [18] Guo, D., Chen, M., Perc, M., Wu, S., Xia, C., Zhang, Y., Xu, P., Xia, Y., & Yao, D. (2016). Firing regulation of fast-spiking interneurons by autaptic inhibition, *Europhysics Letters*, 114, 30001.
- [19] Guo, D., Wu, S., Chen, M., Perc, M., Zhang, Y., Ma, J., Cui, Y., Xu, P., Xia, Y., & Yao, D. (2016). Regulation of irregular neuronal firing by autaptic transmission, *Scientific Reports*, 6, 26096.
- [20] Holt, A. B., & Netoff, T. I. (2013). Computational modeling of epilepsy for an experimental neurologist, *Experimental Neurology*, 244, 75-86.
- [21] Jessberger, S., & Parent, J. M. (2015). Epilepsy and adult neurogenesis, *Cold Spring Harbor Perspectives in Biology*, 7, 1-10.
- [22] Jiruska, P., de Curtis, M., Jefferys, J. G. R., Schevon, C. A., Schiff, S. J., & Schindler, K. (2013). Synchronization and desynchronization in epilepsy: Controversies and hypotheses, *Journal Physiological*, 591.4, 787-797.
- [23] Khajanchi, S., Perc, M., & Ghosh, D. (2018). The influence of time delay in a chaotic cancer model, *Chaos*, 28, 103101.
- [24] Kramer, M. A., & Cash, S. S. (2012). Epilepsy as a disorder of cortical network organization, *Neuroscientist*, 18(4), 360-372.
- [25] Kuramoto, Y (1984). Chemical oscillations, waves, and turbulence. Berlin: Springer-Verlag.
- [26] Li, X., Cui, D., Jiruska, P., Fox, J. E., Yao, X., & Jefferys, J. G. (2007). Synchronization measurement of multiple neural populations, *J. Neurophysiol.*, 98, 3341-3348.

- [27] Lundqvist, M., Compte, A., & Lansner, A. (2010). Bistable, irregular firing and population oscillations in a modular attractor memory network, *Plos Computational Biology*, 6(6), e1000803.
- [28] McCandless, D. W. (2012). Epilepsy: animal and human correlations. New York: Springer-Verlag.
- [29] Naud, R., Marcille, N., Clopath, C., & Gerstner, W. (2008). fire patterns in the adaptive exponential integrate-and-fire model, *Biological Cybernetics*, 99, 335-347.
- [30] Noback, C. R., Strominger, N. L., Demarest, R. J., & Ruggiero, D. A. (2005). *The Human Nervous System: Structure and Function* (Sixth ed.). Totowa, NJ: Humana Press.
- [31] Noachtar, S., & Rémi, J. (2009). The role of EEG in epilepsy: A critical review, *Epilepsy & Behavior*, 15, 22-33.
- [32] Ostojic, S. (2014). Two types of asynchronous activity in networks of excitatory and inhibitory spiking neurons, *Nature Neuroscience*, 17, 594-600.
- [33] Protachevycz, P. R., Borges, R. R., Reis, A. S., Borges, F. S., Iarosz, K. C., Caldas, I. L., Lameu, E. L., Macau, E. E. N., Viana, R. L., Sokolov, I. M., Ferrari, F. A. S., Kurths, J., & Batista, A. M. (2018). Synchronous behaviour in network model based on human cortico-cortical connections, *Physiological Measurement*, 39(7), 074006.
- [34] Rosenblum, M. G., Pikowsky, A. S., & Kurths, J. (1996). Phase synchronization of chaotic oscillators, *Physical Review Letters*, 76(11), 1804-1807.
- [35] Rosenblum, M. G., Pikowsky, A. S., & Kurths, J. (1997). From phase to lag synchronization in coupled chaotic oscillators, *Physical Review Letters*, 78(22), 4193-4196.
- [36] Scharfman, H. E., & Buckmaster, P. S. (2014). Issues in clinical epileptology: A view from the bench. New York: Springer.
- [37] Schindler, K. A., Bialonski, S., Horstmann, M. T., Elger, C. E., & Lehnertz, K. (2008). Evolving functional network properties and synchronizability during human epileptic seizures, *Chaos*, 18, 033119.

- [38] Sierra-Paredes, G., & Sierra-Marcuño, G. (2007). Extrasynaptic GABA and glutamate receptors in epilepsy, *CNS Neurological Disorders Drug Targets*, 6, 288-300.
- [39] Silva, F. H. L., Blanes, W., Kalitzin, S. N., Parra, J., Suffczynski, P., & Velis, D. N. (2003). Dynamical diseases of brain systems: Different routes to epileptic seizures, *IEEE Transactions on Biomedical Engineering*, 50, 540-548.
- [40] Suffczynski, P., Kalitzin, S., & Da Silva, F. H. L. (2004). Dynamic of non-convulsive epileptic phenomena modeled by a bistable network, *Neuroscience*, 126, 467-484.
- [41] Sun, X., Perc, M., Kurths, J., & Lu, Q. (2018). Fast regular firings induced by intra- and inter-time delays in two clustered neuronal networks, *Chaos*, 28, 106310.
- [42] Traub, R. D., Jefferys, J. G. R., & Whittington, M. A. (1994). Enhanced NMDA conductance can account for epileptiform activity induced by low  $Mg^{2+}$  in the rat hippocampal slice, *Journal of Physiology*, 478, 379-393.
- [43] Traub, R. D., Miles, R., & Jefferys, J. G. R. (1993). Synaptic and intrinsic conductances shape picrotoxin-induced synchronized afterdischarges in the guinea-pig hippocampal slice, *The Journal of Physiology*, 461, 525-547.
- [44] Traub, R. D. & Wong, R. K. S. (1982). Cellular mechanism of neural synchronization in epilepsy, *Science*, 216, 745-747.
- [45] Trinka, E., Cock, H., Hesdorffer, D., Rossetti, A., Scheffer, I. E., Shinnar, S., Shorvon, S., & Lowenstein, D. H. (2015). A definition and classification of status epilepticus-report of the ILAE task force on classification of status epilepticus, *Epilepsia*, 56, 1515-1523.
- [46] Uhlhaas, P. J., & Singer, W. (2006). Neural synchrony in brain disorders: relevance for cognitive dysfunctions and pathophysiology, *Neuron*, 52, 155-168.
- [47] Velasco, A. L., Velasco, F., Velasco, M., Trejo, D., Casto, G., & Carrillo-Ruiz, J. D. (2007). Electrical stimulation of the hippocampal epileptic foci for seizure control: A double-blind, long-term follow-up study, *Epilepsia*, 48(10), 1895-1903.

- [48] Wang, Z., Tian, C., Dhamala, M., & Liu, Z. (2017). A small change in network topology can induce explosive synchronization and activity propagation in the entire network, *Scientific Reports*, 7, 561.
- [49] White, H. S. (2002). Animal models of epileptogenesis, *Neurology*, 59, 7-14.
- [50] Wong, M. (2005). Modulation of dendritic spines in epilepsy: Cellular mechanisms and functional implications, *Epilepsy & Behavior*, 7, 569-577.
- [51] Wong, M. (2008). Stabilizing dendritic structure as a novel therapeutic approach for epilepsy, *Expert Review of Neurotherapeutics*, 8(6), 907-915.
- [52] Wu, Y., Liu, D., & Song, Z. (2015). Neural networks and energy bursts in epilepsy, *Neuroscience*, 287, 175-186.